Signal quality improvements by short-coherence holographic particle image velocimetry

Klaus D. Hinsch*, Sven F. Herrmann

Keywords: Particle Image Velocimetry, PIV, particle holography, 3D flow measurement, noise, speckle

Abstract

Particle holography has proven to be a useful metrological tool for three-dimensional flow velocimetry. To cope with the problem of noise from out-of-focus particles the technique of light-in-flight holography (LiFH) has been introduced that utilizes properties of a laser source of short coherence. While the feasibility of the method has been shown earlier, a more profound quantitative analysis of its performance was still required. The present paper briefly summarises some essential knowledge on noise in particle holograms, reviews recent approaches to handle noise in deep-field particle holography and presents first experimental checks of these concepts on short-exposure holographic recordings of particle fields in a wind-tunnel flow. The performance of ordinary and short-coherence particle holography are compared directly by operating the same laser in either long-coherence or short-coherence mode. Some interpretations are checked by continuous-wave recordings in a model environment.

1. Introduction

Recent advances in fluid dynamics ask for metrological techniques to map the three-dimensional velocity field of complex non-stationary flows. Holographic particle imaging velocimetry (HPIV) has been introduced successfully to overcome depth-of-field restrictions of classical imaging techniques (Hinsch 2002). In a holographic recording of a particle field an interference pattern of the light scattered by the particles – the object light – with a reference wave is stored as a hologram. By illuminating the hologram with the reference wave diffraction reconstructs the original object wave. Particle information is then extracted from this wave to obtain position coordinates and displacement data and to calculate velocity vectors. For this purpose, individual particles or particle clusters are localized in two successively recorded holographic images. Usually, both holograms are superimposed on the same carrier material – to be separated by a change in the direction of the reference wave between exposures. When using the real image, the evaluation can be done without any imaging lens. The resolution in the particle images is then set by the effective recording aperture. When the light scattered by the particles covers all of the holographic plate position and size of this plate determine the aperture, otherwise the light-scattering characteristic of the particles must be accounted for.

* Correspondence to: Klaus D. Hinsch
Applied Optics Group, Institute of Physics, Faculty 5; Carl von Ossietzky University, D-26111 Oldenburg, Germany. Phone: +49-441-798-3510; Fax: +49-441-798-3576; E-mail: klaus.hinsch@uni-oldenburg.de

Impressive results have already been obtained by several researchers applying various modifications of the basic holographic set-up. Yet, there remain problems to be solved. One of them is that the maximum size of the field volume is still restricted to a few centimetres in length – mainly caused by the low intensity in the scattered light. During recording, the particle light has to produce a noticeable modulation of exposure in the photographic emulsion. Upon reconstruction, the particle images must be clearly distinguished from any background light to obtain high-validity extraction of displacement vectors. Both requirements are interrelated since a low modulation results in poor diffraction efficiency of the hologram and therefore in weak particle images. The background noise responsible for the signal-to-noise ratio in the final images gets contributions from the unavoidable scattering by the photographic emulsion, but also from out-of-focus particle images as well as from any other neighbouring objects that happened to be recorded in the hologram. The out-of-focus particle images are a special feature of voluminous particle holography since in this case the complete field has to be illuminated – contrary from light-sheet imaging where only a thin section of the whole flow is illuminated. Thus, careful minimization of each of these noise effects enhances the performance of the technique.

Recently, we have introduced several novel versions of HPIV that relax the noise problem. In the first place, for deep-volume particle fields the technique of light-in-flight holography (LiFH) takes advantage of a short-coherent light source to suppress the background light from the large number of out-of-focus particle images (Herrmann *et al.* 2000). Each region on the hologram is responsible for the reconstruction of only a shell in space of limited thickness. By moving along the hologram data from the complete depth can be assembled – each single section, however, without disturbance by particle images from the rest of the field. Secondly, the weak light scattering by particles and the resulting low object-to-reference beam ratio and poor diffraction efficiency are compensated for by a long-exposure extraction of the particle information from the reconstructed real image (Herrmann and Hinsch 2001). The limit to this procedure, however, is set by the background noise terms. Therefore, an overall estimate of the performance of these methods requires a thorough experimental analysis of the noise situation in these types of particle holograms.

As mentioned, the essential parameter in HPIV is the hologram aperture, i.e., the solid angle covered by the area on the hologram contributing to the reconstructed particle image. Its influence is threefold. First of all, it determines brightness and resolution of the particle images. The larger the aperture the more light goes into the particle image and the better the resolution governed by diffraction. As a consequence, designers of holographic systems usually strive to collect scattered light from the particles over as large an angular region as possible, for example by using a large hologram. Experimental limits to this aim, however, are set by uneven light-field over the cross-section of the reference beam or by variations in the response of the photographic emulsion – an issue to which we will return. In LiFH different regions on the hologram are assigned to record different depth sections from the object volume and thus the effective aperture is restricted in size to just a fraction of the complete hologram. Due to this counteracting dependence all effects need a thorough study and the proper aperture size must be selected quite carefully.

The present paper briefly summarises some essential knowledge on noise in particle holograms, reviews recent approaches to cope with noise in deep-field particle holography and presents experimental checks of these concepts on short-exposure holographic recordings of particle fields in a wind-tunnel flow. The performance of ordinary and short-coherence particle holography are compared directly by operating the same laser in either long-coherence or

short-coherence mode. Some interpretations are checked by continuous-wave recordings in a model environment.

2. Light-in-flight experiments

Let us briefly repeat the basis of light-in-flight particle holography. Holography relies on the interference of object and reference wave at the position of the photographic plate. The resulting intensity modulation is recorded, serves as a complicated diffraction grating during reconstruction and causes light from the reference beam to rebuild the object wave. The example of Fig. 1 (left) illustrates the schematic recording set-up. A collimated reference wave obliquely incident from the left superimposes on the photographic plate with light scattered by the particles. A successful holographic recording requires that the path-lengths travelled by either wave differ by no more than the coherence length L. In the present case, the reference wave has travelled a longer path to the right side of the holographic plate than to the left. Similarly, the light from the far-off particles has travelled farther than from those close by – which is purposely enhanced by illuminating the particle field from a direction close to the viewing direction. Thus, for sufficiently short coherence and with proper alignment, particles from a shell in the middle of the observed field are recorded in a small region in the middle of the plate, particles from a front shell on the left and from a rear shell on the right.

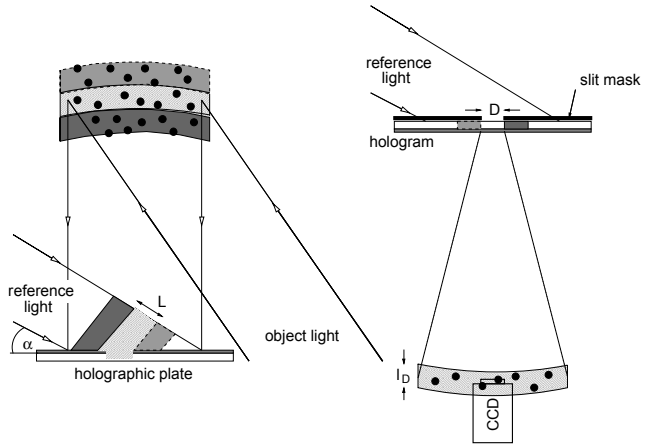

Figure 1: Schematic of set-up for recording light-in-flight holograms of particle fields and reconstructing real particle images. The finite coherence length L restricts holographic recording to a field limited in depth. Its location depends on the position of the aperture on the hologram.

The second step in holography is the reconstruction of the object wave. For this purpose the hologram is illuminated with the original reference wave to produce a virtual image of the object. When, instead, a phase-conjugate version of the reference wave is used a real image is reconstructed in space that can be picked up directly on a CCD-sensor. In the present case of a plane parallel reference wave it suffices to illuminate the hologram from the back which can be achieved by turning it through 180° – seen in Fig. 1 (right). As a consequence of the light-in-flight recording, a limited-area aperture on the hologram (let it have the size D along the hologram direction) will reconstruct only particle images within a shell of a depth of roughly one half $(D + L)$ – the precise value depends on the shape of the aperture, the illumination

direction and the angle of incidence of the reference wave. To reconstruct other regions we have to move the aperture from left to right in the plane of incidence. The great advantage is that out-of-focus particles from regions outside the shell – and these will be the more the deeper the volume – will not disturb the image under investigation.

Let us demonstrate these characteristics of LiFH with a set-up that has been developed for the study of flow fields in a wind-tunnel environment (Herrmann and Hinsch 2003). A holographic plate 0.12 m in width is placed some 0.35 m from the centre of the flow region of interest. The particles – DEHS of about 1μm diameter – are illuminated from a direction about 30° off the viewing axis to the centre of the hologram, i.e., we are operating in the near-backscattering regime. The reference wave is incident at about 20° with the direction of the plate. With both angles being so small they can be disregarded in the path length calculations. The recording is done at a wavelength of 532 nm by a frequency-doubled Nd:YAG-laser that provides light pulses of about 7 ns duration and 1.5 J energy. For flow-analysis applications the laser system (that actually consists of two lasers) can be operated in a double-pulse mode to obtain two successively recorded holograms that are distinguished by the direction of their reference waves. In the present analysis of image quality it is sufficient to investigate single-pulse holograms. The coherence properties of the laser can be changed from a long-coherence single-mode operation – seeder-laser turned on, coherence length almost 2 m – to a short-coherence multi-mode operation which provides a coherence length of about 7 mm. Thus, it is easy to compare the particle image properties under conditions of "ordinary" holography with those under light-in-flight conditions – simply by turning the seeder on and off.

For the reconstruction, the hologram is illuminated with a well-adjusted phase-conjugate, i.e., backward-travelling green reference wave from a cw 150-mW Nd:YAG-laser to produce a real particle-image field that is interrogated by a bare CCD-target containing 1280×1024 pixels which corresponds to a viewing field of 8.5×6.9 mm^2. Data about the complete flow volume are accumulated by scanning the CCD through 3-D space. For the present investigations, a circular aperture of varying diameter is moved across the hologram to reconstruct different regions in depth and the CCD-sensor is scanned along the depth coordinate to probe the particle-image field. The spatial configuration allows to view a field of illuminated particles of about 5 cm in depth from any location on the hologram. Such a deep-volume situation may now be compared with the sheet-like situation of LiFH where the reconstructed field is only several millimetres in depth.

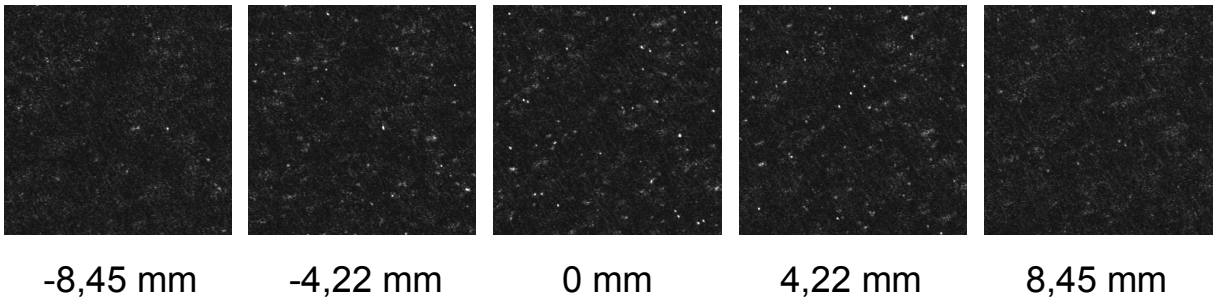

Figure 2: Real-image holographic particle records obtained on a CCD-sensor from a light-in-flight hologram of a wind-tunnel flow. While the reconstructing aperture of 20 mm diameter was kept fixed on the hologram, the pictures were obtained at different depth positions of the sensor. The position of the centre image corresponded to zero path-length difference Δs between object and reference light. Indicated are the values Δs for the different images. Field of view 300px×300px (2×2 mm^2).

Typical features of a reconstruction of particle images from a light-in-flight hologram are illustrated in Fig. 2. We select a central position of the aperture (D = 20 mm) on the hologram

and place the CCD-sensor at such a depth location that the difference in path length Δs between object and central reference light is zero. To investigate the extension in depth of the reconstructed field we now move the sensor along the depth coordinate z. Results for five positions are shown. It is clearly seen that the central location produces a high-quality image with many clearly distinguishable particle images and that at positions in the front and back the image intensity decreases. When the path length difference with respect to the centre of the volume is raised to about 8 mm there are hardly any particle images left which is in good accordance with predictions from coherence length and aperture diameter. Since the essential parameter is the difference in path length, similar results are obtained when the sensor position is kept fixed (constant object light path) and the aperture is moved to change the length of the reference light.

The short-coherence version of particle holography has been introduced to eliminate the disturbing influence of the large number of particles from the field depth – in the present case approximately 5 cm. We can nicely demonstrate the improved quality by comparison with images from a hologram that has been taken in the same set-up, but in the long-coherence operation (seeder turned on). In Fig. 3 we compare a zero path-length picture from the long-coherence case with the corresponding image of the short-coherence hologram (aperture diameter D = 15 mm in either case). Unfortunately, the original pictures to compare differed in brightness because the experimental parameters during the recording were difficult to control. For purposes of better comparison in the presentation we have thus enhanced the low-coherence picture by a factor 3 which equalizes the brightness of the in-focus particle images of both the pictures. It is clearly seen that the long-coherence image is affected by more noise originating from the of out-of-focus particle images that superimpose for a speckle-like background. In the following analysis this situation is investigated in more detail to understand the physics involved and to quantify the improvement.

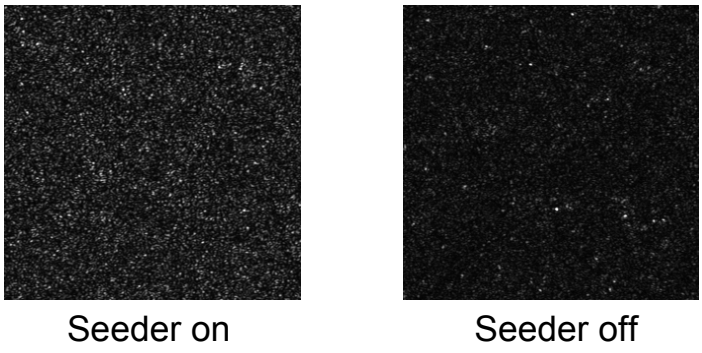

Figure 3: Comparison of reconstructed images at zero path-length difference for (a) ordinary long-coherence hologram and (b) light-in-flight hologram (short coherence). Field of view 300px×300px (2×2 mm^2).

3. Noise in off-axis real-image particle holography

3.1 Emulsion Noise

The inevitable source of noise in the holography of deep-volume particle fields are out-of-focus particle images. We have seen that these set a limit to the depth of the measuring volume or to the particle number density when traditional particle holography is employed. To

gain an impression of the extent of this effect we need to separate it from other noise sources. The dominating competing noise is produced by scattering from the film grains in the emulsion. In the bright holograms of ordinary holography this noise is of negligible concern – not so when weak particle images are to be reconstructed. Experimentally, emulsion noise can be easily separated from other noise contributions by observation of a region in image space that does not contain any object light.

The theory for this type of noise is well-established, various models have been applied for different purposes. Emulsion noise results from a random superposition of many coherent contributions scattered by photographic grains and thus follows speckle characteristics. This is independent of the type of model used – Goodman (1967), for example, elaborates a checkerboard and an overlapping circular-grain model. In any case, average noise intensity $< I_N >$ increases proportional to the reconstructing hologram area A_H (aperture). This result is easy to understand since the contributions from different regions on the aperture add with random phases.

We have evaluated emulsion noise for the particle holograms from the wind-tunnel flow. Particle images are reconstructed in a limited region in space only, corresponding to the flow section originally illuminated. For emulsion-noise measurement the CCD-sensor is therefore displaced transversally from the flow region – just enough to move outside the reconstructed image light. Thus we avoid any light of the holographic image and expect only light scattered from the plate. To check reproducibility two positions are chosen for the CCD, one is adjacent to the particle field under a slightly larger angle than the direction between reconstructing wave and the light to the flow field image, the other at a slightly smaller angle. CCD-images are taken for different sizes of the reconstructing circular aperture on the hologram (diameter D). For an evaluation the total averaged (noise) intensity is calculated from an addition of the grey-tone values of all pixels in the recorded CCD-image. This is done for two holograms, the long-coherence hologram of ordinary holography and the short-coherence hologram of light-in-flight operation. Mind that the optical set-up is identical in both situations.

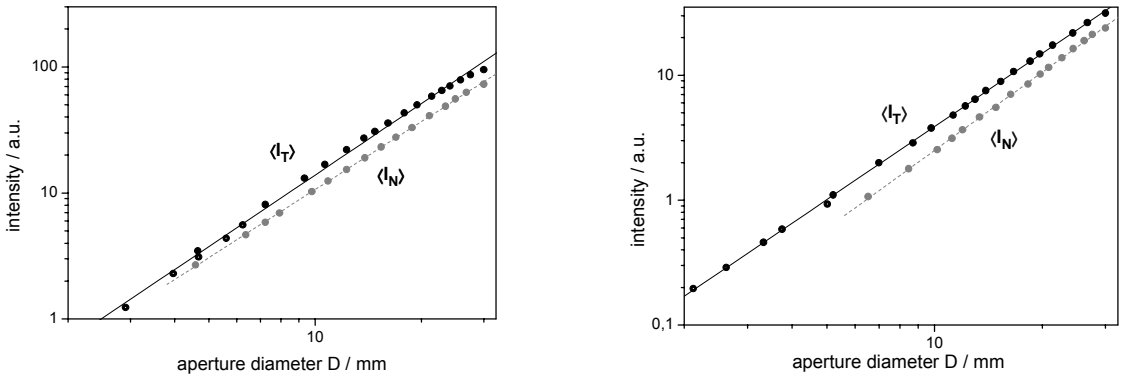

Figure 4: Average emulsion noise $< I_N >$ and total image intensity I_T versus diameter of the hologram aperture for the long-coherence (a) and the short-coherence case (b).

In comparing noise data from both the measuring positions the position further off in angle from the reconstructing light yields slightly lower values. This is reasonable, because the scattering intensity usually decreases towards higher spatial frequencies – as expressed by the Wiener spectrum of the emulsion (Kozma 1968). The following results have therefore all been accumulated at one position. In Fig. 4a and Fig. 4b, the noise intensity $<I_N>$ is plotted in

a double-logarithmical representation versus aperture diameter D for both the long-coherence and short-coherence case, respectively. For the total intensity values see a later chapter. Both graphs follow an almost linear shape, the slope can be approximated by roughly 1.8 and 2.1, respectively. This is a good demonstration of the validity of the random nature of the generating process. The slight deviation from the expected proportionality to the aperture area (slope of 2.0) can be explained by individual characteristics in each hologram. A visual inspection of the holograms reveals non-homogeneous exposure due to intensity irregularities in the beam cross-section of the high-energy laser. The transmittance of the developed emulsion differs considerably already within one hologram. Thus, when the hologram aperture is enlarged, the added area may differ somewhat in scattering. Also, a direct comparison between different holograms is not directly possible which is obvious from the difference in absolute noise values between the holograms.

We carried out another check as to the nature of emulsion noise. When this is explained by a speckle-oriented generation process, the standard deviation σ in the light field should be equal to the average intensity $< I_N >$. We calculated σ from the pixel data and found that, first of all, the ratio $\rho = < I_N > / \sigma$ is not equal to unity and, secondly, that it is not even constant but increases slightly and almost linearly with diameter D. For the long-coherence case, ρ runs from 1.2 to 2.0, for the short-coherence case from 1.6 to 2.4. This observation, however, does not question the speckle model. We have to take into account that the noise data are obtained from spatially integrated samples due to the finite size of the pixels on the CCD array. This averaging is more pronounced for small speckle, i.e., for large apertures. Since it smears out the modulation in the light field we measure reduced values of σ with increasing aperture diameter D and thus higher values for ρ. Indeed, for an aperture diameter of 30 mm we expect an average speckle size of about 7 µm – almost the same value as pixel size and thus of the right order of magnitude to produce an effect. A detailed analysis could be based on Godman's fundamental speckle treatment (see Equ. 2.111 in Goodman 1984) which shows that ρ is equal to the square root of a parameter M which is a monotonous function of the number of speckle correlation cells within the integrating aperture.

Emulsion noise is also crucial in the extraction of rather dark particle images by long-exposure recording. Due to the weakly scattering small tracer particles of particle velocimetry it is usually difficult to achieve conditions for optimum holographic recording. A bright holographic image requires high modulation in the transmittance of the developed photographic plate for which purpose the object-to-reference intensity ratio should be about 0.2 – impossible to achieve in larger measuring fields. A solution is to accept the low light level in the reconstructed particle images and register them by a long-exposure recording. A basic limit to this procedure, however, is the ever present emulsion noise which is fairly independent of the object intensity and sums up with exposure time. An experimental investigation of this method has verified the theoretical concepts for emulsion scattering (Herrmann and Hinsch 2001) as have earlier studies in which a single point source was recorded holographically (Meng and Hussain 1995).

Let us repeat that emulsion noise is just one source disturbing the quality of the reconstructed particle images. However, it is the part that can be separated most easily. In the reconstructed light field there will be additional contributions that originate from out-of-focus particle images and other sources of accidental background light that happened to be recorded on the hologram. While the latter part should be minimized by careful check of the optical set-up the former is inherent to the holography of a deep-volume particle field. It is this part that shall be reduced by the light-in-flight recording. We will now attempt to determine the extent of the

additional noise sources by a more detailed study of the contributions to the holographic image.

3.2 Signal-to-noise ratio in particle-field images

In our study we would like to compare the performance of different approaches in particle holography. The quality of the reconstructed images can be quantified by a value for the signal-to-noise ratio SNR. Here, SNR is defined as the ratio of the deterministic image intensity I_i – the particle images – to the standard deviation σ of the total image intensity I_T. Towards this aim we need to know which part in the total intensity is due to the particle images. This is inherently difficult, because we have to distinguish between particle images of different quality. There are well-focused images useful for the displacement analysis of holographic particle image velocimetry and totally out-of-focus images that must be considered noise. Of course we encounter also all intermediate states. To understand the dimension of the problem we have to recall further that contributions from the various sources listed earlier add on an amplitude basis and thus interfere to produce the total image intensity in the reconstructed image.

For a simple basic approach to outline the situation we assume that all noise shows speckle properties. The total intensity is then calculated as (Godman 1967, appendix B)

$$\left\langle I_T^2 \right\rangle = I_i^2 + 4 I_i \left\langle I_N \right\rangle + 2(\left\langle I_N \right\rangle)^2 . \tag{1}$$

from which we also obtain a formula for the standard deviation σ of the total intensity

$$\sigma = \left\langle I_N \right\rangle \left[1 + \frac{2 I_i}{\left\langle I_N \right\rangle} \right]^{1/2} . \tag{2}$$

Thus, we get the relation for SNR

$$\frac{I_i}{\sigma} = \frac{I_i / \left\langle I_N \right\rangle}{(1 + 2 \frac{I_i}{\left\langle I_N \right\rangle})^{1/2}} . \tag{3}$$

SNR turns out to be a monotonically increasing function of $I_i/\langle I_N \rangle$ where two simple limiting cases apply for relatively large and small noise (Godman 1967). Our application in flow diagnostics requires successful particle discrimination and thus scores under conditions of low noise – the generally accepted value for good-validity results is SNR > 5. In this case the influence of the noise becomes overemphasized due to interference. For an example a 10% amplitude noise will produce fluctuations in total signal level between 80% and 120% .

The small noise treatment yields a final formula for SNR

$$\frac{I_i}{\sigma} = \left[\frac{I_i}{2 \left\langle I_N \right\rangle} \right]^{1/2} . \tag{4}$$

Mind that the image intensity I_i in these relations is not available from our records. Though we can try to separate particle images from the background by a threshold criterion we meas-

ure only the intensity after interference of the image light with the coherent background. In absence of any better means, however, we will have to disregard this effect.

Let us now obtain more data from our particle image fields. Using the same holograms as before we now turn to regions where we find the field of real particle images from the flow. First of all, we determine the total integrated intensity $< I_T >$. This quantity is measured as before by summing the grey values – now, however, we place the CCD array within the particle-image field to obtain images of the type shown in Fig.2. The position of the aperture is also as before and once more we increase its diameter. The results for both conditions of coherence have been added to the emulsion data in Fig. 4a and Fig. 4b. The plots indicate, that the averaged total intensity, i.e., the sum of holographic image plus emulsion noise, follows a slope of about 1.9 and thus also increases approximately proportional to the aperture area used for reconstruction. The slight deviation from a value of 2 can be explained as before. This result is independent of the type of hologram – long or short coherence.

Next, the standard deviation σ of the total intensity is extracted from the CCD-records. It is determined over all pixel values, including those that obviously belong to particle images. By the way, it was shown that the values obtained in such a way do not differ much from results that disregard the particles – which is obvious because the number of particles is low. Results for σ are given in Fig.5 in logarithmic scales for both coherence cases. Roughly, σ grows with aperture diameter fairly much like $D^{1.5}$. This is true independently of long coherence length (fit in the logarithmic plot yields an exponent 1.49) or short coherence length (exponent 1.62).

To determine a value for SNR from our data we need the intensity of the particle images I_i. This shall be set in relation to the standard deviation as required by the definition of SNR. We have mentioned earlier that this value is not directly available from our images due to interference with the background. All we can do is to extract particle image data from the records by masking "particles", a procedure that has been applied similarly in earlier studies (Meng *et al.* 1993). For this purpose we define a proper threshold value, consider all area with intensity above the threshold as particles and average the grey-tone values of these regions. Of course, there is some arbitrariness in assigning the threshold, the more as the particle image changes in size with changing aperture diameter. We have selected the threshold by visual inspection of the grey-level histograms of the pictures. The results have been included in Fig. 5. For both cases of long coherence (exponent 1.47) and short coherence (exponent 1.49) the particle image intensity thus calculated once again increases with a slope of about 1.5, fairly parallel to the σ-plots.

Now it is just a straightforward division to get values for SNR as shown in Fig.6. For the "ordinary" hologram we find SNR ≈ 8 independent of aperture diameter. For the short-coherence LiF-hologram we observe a clearly improved SNR ≈ 15 that stays constant up to about $D_0 \approx$ 15 mm and then drops gradually. The drop is quite plausible from the special features of light-in-flight holography. The depth location of the CCD-sensor has been chosen such that it corresponds to the central position of the aperture. Now, only light from within an aperture of approximately twice the coherence length in diameter participates in producing the particle images. For a while – when opening the aperture – additional area on the hologram contributes to the reconstruction of the particle images on the CCD. When the coherence limit is reached, however, new aperture area no longer contributes to the brightness of these particles – just this is the principle of LiF-holography. On the other hand, the contribution from noise continues to increase. The real situation is a little more complicated, because only the dimension of the aperture parallel to the plane of incidence is affected in this way, while the other

direction still carries particle information. Furthermore, coherence does not drop abruptly thus explaining the gradual decrease of SNR.

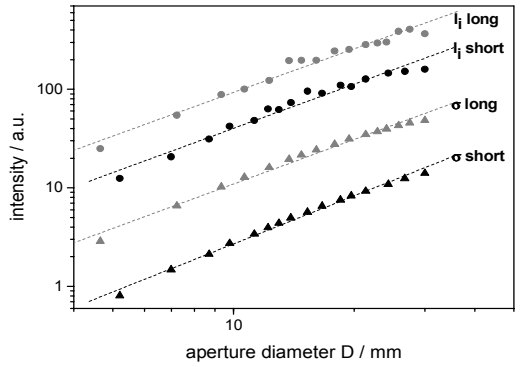

Figure 5: Standard deviation σ of total intensity and image intensity I_i versus diameter of the hologram aperture for both the coherence cases.

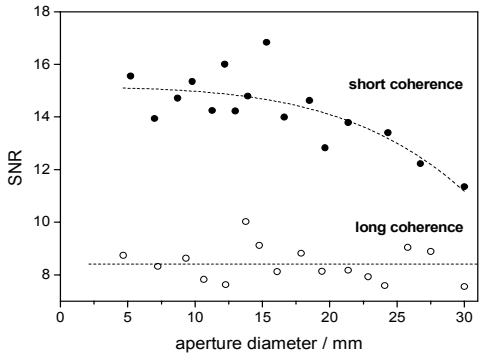

Figure 6: Signal-to-noise ratio SNR in real particle-image fields reconstructed from ordinary long-coherence and light-in-flight holograms versus diameter of the hologram aperture. Both the measurements were made under identical conditions, they differ only in the activation of the Nd:YAG-laser seeder for the long-coherence case.

In the present situation, LiF-holography has thus brought a gain in SNR by a factor 2. The physical reason is the suppression of out-of-focus light from a column of particle images several centimetres in length. It would be interesting to compare this finding with other consequences from signal deterioration by out-of-focus noise. For example, in a numerical simulation it has been determined how the validation rate in PIV decreases with increasing depth of the particle field (Hinrichs *et al.* 1998). To compare this to our results, however, validation rate needs to be related to SNR for which numerical modelling might be appropriate.

3.3 Comparison with theory of holographic image intensity

Our investigations indicate that in particle holography under conditions for holographic velocimetry SNR is independent of the size of the effective hologram aperture. In the following we would like to link this finding to a theoretical model about holographic imaging. We derive the basic explanation from the coverage by Godman (1967) and need not to go into the details of later refinements for other purposes (Kozma 1968, Meng and Hussain 1995). Besides modelling the emulsion noise – which we have already used earlier – Godman's study also derives an expression for the holographic image intensity I_i in the reconstructed real image of a light-scattering object. It turns out that this quantity is proportional to the exposure E_σ from a resolution cell arriving at the holographic plate and to the square of the hologram aperture area A_H. The resolution cell, of course, is defined by the shape and size of the hologram aperture which means that all light from the cell is, indeed, collected on the hologram. Recall that the resolution cell can not be distinguished from an ideal point source, because the light from either arrives as a spherical wave all over the hologram area.

This general result is then elaborated for two extreme cases:

First an isolated point-source object is covered. Particle holography fits in this situation under the following assumptions: Let us assume that the particle distribution in space is not very dense and that particles are always smaller than the resolution cell, i.e., the size of particle images is completely determined by diffraction-limited imaging. Further, we disregard that part of the hologram aperture area may not be involved in recording the particle wave due to the angular characteristics of light scattering.

In this case, because exposure E_σ is independent of the size of the resolution cell, we arrive at $I_i \propto A_H^2$. Since $< I_N > \propto A_H$ we obtain $I_i/< I_N > \propto A_H$. If we recall the square-root relation Equ. (4) between signal-to-noise ratio and this ratio for the small-noise case we end up with

$$\frac{I_i}{\sigma} \propto \sqrt{\frac{I_i}{\langle I_N \rangle}} \propto \sqrt{A_H} \propto D \,. \tag{5}$$

Let us add a comment to the remarkable result that the image intensity increases proportional to $A_H{}^2$ which, of course, is a consequence of the coherent superposition of partial amplitudes from hologram sub-areas. More precisely, the image light is contained in the resolution cell as determined by the hologram aperture. At first glance it seems to violate energy conservation that we find four-times the intensity when we double the hologram aperture. Mind, however, that this light is now concentrated on a smaller resolution cell and the rest of the former has become dark – which re-establishes the energy principle.

This consideration introduces the second case treated, a diffusely reflecting surface. Obviously, we have a continuous multitude of unresolved scatterers where the energy density responsible for the exposure E_σ is proportional to the area of the cell, which in turn decreases with A_H. Thus image intensity goes proportional to A_H and signal-to-noise ratio is independent of the hologram aperture. Here, the energy principle is straightforward, contrary to the earlier case there are no regions that can compensate for the increase in image intensity by getting dark.

The result from the experimental investigations is in favour of the second case. Apparently, an ensemble of scattering particles closely packed over a certain depth in space approaches the case of a diffusely scattering particle cloud. We still can resolve particles, yet the field gets dense due to the projection of out-of-focus particles into the plane of reference. A close look at details of our earlier results, however, reveals that I_i as well as σ do not increase like D^2 but rather like $D^{1.5}$. Since both do the same, this does not show up in the result for SNR, however there is a clear difference from the theoretically expected exponent of 2. We must therefore recall those approximations mentioned earlier for which the model presented here is rather simple. For further elaboration, three effects should be considered predominantly:

1. The properties of the laser reference beam may not be sufficiently controlled to guarantee the phase-conjugate reconstructing wave. The recording was done with a high-energy pulsed Nd:YAG laser whose collimated reference beam definitely showed cross-sectional variations in wave intensity. We can assume that there will also be corresponding phase fluctuations. In the reconstruction a high-quality cw Nd:YAG laser was used. Different sub-areas on the hologram will then superimpose with the wrong phase relation and reduce the effects of coherent superposition.
2. Inhomogeneities in the index of refraction and the surface profile of the photographic layer – consequences of the chemical processing – will produce similar effects. While we

have not taken any special precautions in this study, in the past much effort has been dedicated to avoid such effects (Barnhart *et al.* 1994).

3. Particle scattering is dominated by pronounced angular intensity variations. Different regions on the hologram will thus get quite different amounts of particle light – contrary to our assumption that all of the hologram area will be treated equally.

The first suspicion has been checked by an experiment using the cw Nd:YAG-laser both for recording and reconstruction. A model particle field of 10µm PMMA particles in a perspex block is illuminated with a thick light-sheet (4-8 mm) to provide conditions as in LiFH. Here we have recorded the light scattered at 90° – which, however, is of no importance for the present situation. Once again, the real particle images are evaluated by CCD as in our earlier experiments. The average particle intensity I_i extracted from these records as plotted versus D shows, indeed, a steeper slope which is close to the expected value 2 and thus supports our assumption. A final proof would require laborious tests on the laser light. Both the other effects are well-known and would need further elaboration to fit into the present analysis.

4. Conclusions

We have been concerned with the reduction of noise in the holographic study of voluminous particle fields for flow velocimetry. This noise originates from out-of-focus particle images the number of which increases with particle number density and volume depth. A plausible remedy has been introduced, i.e., light-in-flight holography where a large part of this noise can be suppressed by making use of the short coherence length of the laser source. However, an essential consequence in LiF-holography is a reduction in the effective hologram aperture. Since the aperture size is closely connected to image brightness and resolution this situation required closer investigations.

We are now in a position to comment on our initial concern that the reduced aperture size might compensate the beneficial reduction in background noise. Our investigations have shown that the intensity of the particle images does not increase proportional to the square of the aperture size as we should expect for fully coherent superposition in a field of clearly distinguishable particle images. Thus SNR is not improved by increasing the aperture. And within the limits set by the coherence length, the light-in-flight arrangement provides a clear gain in SNR. While the present experimental conditions did not fully comply with the assumptions used by the theoretical predictions we nevertheless gained insight into the physical situation responsible for image quality in particle holography.

References

Barnhart D H, Adrian R J, Papen G C (1994) Phase conjugate holographic system for high resolution particle image velocimetry. *Appl. Opt.* **33** 7159-7170.

Goodman J W (1967) Film-grain noise in wavefront-reconstruction imaging. J. Opt. Soc. Am. **57** 493-502.

Goodman J W (1984) Statistical properties of laser speckle patterns. In Dainty J C (ed.): *Laser Speckle and Related Phenomena*. Springer Verlag, Berlin, pp 9-76.

Herrmann S F, Hinrichs H, Hinsch K D and Surmann C (2000) Coherence concepts in holographic particle image velocimetry. *Exp. Fluids* **S** 108-116.

Herrmann S F and Hinsch K D (2001) Particle holography and the noise limit. (CD-Rom) *Proc. 4th Int. Symp. On Particle Image Velocimetry (Göttingen) paper* 1021.
Herrmann S F and Hinsch K D (2003) Light-in-flight holographic PIV (LiFH-PIV) for wind-tunnel applications: off-site reconstruction of deep-volume real particle images. *Proc. Workshop on Holographic Metrology in Fluid Dynamics*, Loughborough 2003.
Hinrichs H, Hinsch K D, Kickstein J and Böhmer M (1998) Deep field noise in holographic particle image velocimetry (HPIV): numerical and experimental particle image field modelling. *Exp. Fluids* **24** 333-9.
Hinsch K D (2002) Holographic particle image velocimetry. *Meas. Sci. Technol.* **13** R61-R72.
Kozma A (1968) Effects of film-grain noise in holography. *J. Opt. Soc. Am*. **58** 436-438.
Meng H, Anderson W L, Hussain F and Liu D D (1993) Intrinsic speckle noise in in-line particle holography. *J. Opt. Soc. Am*. **A10** 2046-2058.
Meng H and Hussain F (1995) In-line recording and off-axis viewing technique for holographic particle velocimetry. *Appl. Opt.* **34** 1827-1840.

Acknowledgement

We acknowledge financial support by the EU through grant G4RD-CT-2000-00190 (EUROPIV2).